FReET-D: Deterioration Module
of the Multipurpose Probabilistic Software
for Statistical, Sensitivity and Reliability Analysis FReET

DEMO VERSION

http://www.freet.cz/download.html

The demo version of FReET-D is compatible to the both demo and sharp version of software FReET. When using demo version of FReET only the uniform distribution functions are available for the calculations.

Distributor: Červenka Consulting
http://www.cervenka.cz

Written by:

Dita Vořechovská, Pavel Rovnaník, Břetislav Teplý and Markéta Chromá

Brno, September 2015

Contents

1 INTRODUCTION **2**
1.1 Safety formats . . . 2
1.1.1 Service Life Format . . . 2
1.1.2 Limit State Format . . . 3
1.2 Objective of the program . . . 4

2 CARBONATION OF CONCRETE **5**
2.1 Limit-state functions . . . 6
2.2 Carbonation models . . . 6
2.2.1 Carb1a . . . 6
2.2.2 Carb1b . . . 7

3 INGRESS OF CHLORIDE IONS **8**
3.1 Limit-state functions . . . 9
3.2 Models for chloride ingress . . . 9
3.2.1 Chlor1a . . . 9

4 EXAMPLES **11**
4.1 Example 1 . . . 11
4.2 Example 2 . . . 25

References **27**

1 INTRODUCTION

Integrated Design and its subset, *Performance-Based Design* (PBD) are leading trends in structural engineering design at present; these approaches deal with *durability* and *reliability* issues, both of which are among the decisive structural performance characteristics. More specifically:

Assessment, together with inspection, maintenance and/or reconstruction plans, must guarantee the correct performance of a structure during its intended or residual service life. This time, t_S, is defined as the assumed period of time, for which the structure will continue to serve its purposes. The intended service life, agreed by the client and justified on the basis of socio-economic criteria, is the design life t_D. This is decided on a case by case basis.

A design or assessment process must always define: (i) the reliability (or safety) level of the relevant limit states; (ii) the service life inherent to the final results; (iii) the conclusions and possible optimization to be carried out for the structure under consideration.

1.1 Safety formats

The safety formats which are commonly used in structure engineering for the purpose of design or safety assessment are based on the concept of limit states. Conceptual models used for this consideration include load transfer, based mainly on statics and dynamics, and the mechanisms of changes in stress and strain fields (yielding, crushing, buckling, cracking or deformation) resulting in failure - more generally: the loss of required performance. The same concept applies to **durability**: the conceptual models for durability relate to the mechanisms that transform environmental actions (performed over time) into cumulative, time-related degradation that results in damage mechanisms causing failure (the loss of required performance).

Traditionally, when dealing with design issues, the main attention is focused on mechanical design, because of structural safety reasons and the serious consequences of structural failure for human beings. However, degradation and obsolescence together are the most important causes of the need for refurbishment or demolition, and therefore have great economic consequences. Therefore, it is important to develop rational and systematic methodologies and methods for controlling all these types of limit states in the lifetime planning, design and management processes for civil infrastructures.

Suitable methods for the monitoring and reliable mathematical modelling of associated effects are needed - better knowledge in this respect provides the basis for a practical and proactive strategy when designing and maintaining concrete structures. This is also reflected in recent international standards and documents - e.g. [5] and [9] and the trend is fully employed in FReET-D. Two safety format categories may be considered: Service life format and Limit state format.

1.1.1 Service Life Format

The service life format consists of determining the remaining design service life, t_D, of a component or structure, by assessing its predicted service life, t_S. The predicted service

live, t_S, of the structure and its components should meet or exceed their design live, t_D, i.e.

$$t_S \geq t_D \tag{1}$$

Within the probability framework: the following probability is compared to a specified target probability

$$P\{failure\} \text{ at } t_D = P\{t_S(X_i, t) < t_D\} \leq P_{target} \tag{2}$$

The t_S is a predicted value modeled as a function of basic variables, X_i and t.

In the case where a structural component is protected against degrading agents (e.g. the concrete cover of reinforcement, the zinc coating of steel), t_S can be determined as a sum of two service-life predictors (often called the initiation period and the propagation period), see also Fig. 1:

$$t_S = t_i + t_p \tag{3}$$

where t_i, the time to the initiation of degradation, is modeled as a function of the basic variables for agent transfer, X_i and t. Time t_p, the service life after the initiation of degradation (the propagation period), is a function of certain basic variables for damage or resistance and t. Basically, the variables X_i are random variables, though some of them might be treated as deterministic values in certain situations. It should be recognized that the service lifef t_S can be considered as a random variable having its own probability density function.

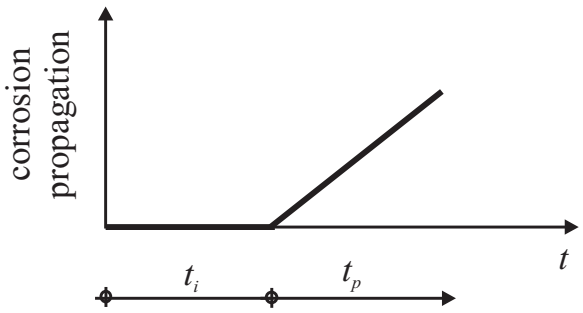

Figure 1: Exposure time periods.

1.1.2 Limit State Format

Ultimate Limit State: The basic requirement for the ultimate limit state during the design service life of the component, t_D, is

$$R(t_D) \geq S(t_D) \tag{4}$$

where $R(t_D)$ is the resistance capacity of the structural component at the end of its design life, t_D, and $S(t_D)$ represents the cumulative degradation of the component at the end of

its design life, t_D. $R(t)$ and $S(t)$ are modeled as functions of the basic variables, X_i and t. The ULS condition, Eq. (4), is ensured by checking that

$$P\{failure\} \text{ at } t_D = P\left\{R\left(t_D\right) - S\left(t_D\right) < 0\right\} \leq P_{target} \tag{5}$$

Either the resistance R or the load action S or both can be time-dependent quantities. Thus the failure probability is also a time dependent quantity. The above formulation applies to material deterioration and deformation which is cumulative, and, in cases where the functions R and S are considered to be monotonous.

Serviceability Limit States: The basic requirement for the serviceability limit states during the residual design life of the component, t_D, is

$$S(t_D) \ \geq \ S_{lim} \tag{6}$$

where S_{lim} represents the serviceability limit. The SLS condition, Eq. (6), is ensured by checking that

$$P\{failure\} \text{ at } t_D = P\left\{S_{lim} - S\left(t_D\right) < 0\right\} \leq P_{target} \tag{7}$$

In several SLS situations it might be advisable to use a conservatively defined limit state expressed by the simplified equation Eq. (8) instead of Eq. (3):

$$t_S \ = \ t_i \tag{8}$$

This kind of limit state precedes the occurrence of other SLSs or ULSs and represents a simplified limit state intended to prevent the onset of deterioration; it is based on the initiation of deterioration and will be called a Durability Limit State (DLS).

Note: Apart from the probability of failure the **reliability index** β can be used as an alternative, with both values being related by the formula

$$\beta = -\phi^{-1}(P\{failure\}) \tag{9}$$

where ϕ is the cumulative distribution function of the standardized Normal distribution.

1.2 Objective of the program

Unfortunately, the prescriptive approach of current standards (Eurocodes) does not allow for design focused on specific service life and/or a specific level of reliability. Therefore, the utilization of stochastic approaches (a combination of analytical models and simulation techniques) and specialized software tools for assessing newly designed as well as existing concrete structures is needed. **FReET-D** provides:

1. modelling of degradation phenomena in concrete structures, and statistical and sensitivity analyses;
2. assessment of service life;

3. assessment of reliability measures.

For the purposes of options 2 and 3 the user may create different simple limit conditions, e.g. the evaluation of service life could be based on Eq. (6):

$$carbonation\ depth\ =\ concrete\ cover\ thickness \tag{10}$$

Thus, FReET-D provides a tool necessary to perform design or safety assessment under the safety formats described above. The name of the software reflects the purpose and strategy: **FReET-D** is the acronym for **F**easible **RE**liability **E**ngineering **T**ool for **D**egradation effects assessment.

FReET-D is developed on the basis of the multipurpose probabilistic software FReET. It might be useful to consult the FReET manuals about simulation techniques, statistical sensitivity, and reliability analyses, and the statistical dependence of variables [18].

The input data for FReET-D are considered to be statistically independent random variables (optionally the deterministic values for individual variable may be chosen too; in special cases the statistical dependence of mutual variables may also be treated). In this way, the inherent uncertainties in inputs are accounted for and via statistical analysis (utilizing simulation techniques) the realistic scatter of output values is assessed; the **randomised form** of all degradation effects is introduced.

Degradation models are time dependent mathematical functions that show the average increase of degradation with time. These models are parameterized with several material, structural and environmental parameters. The main criteria in selecting the degradation model for each specific use are e. g.:

- type of relevant limit state and exposure conditions;
- availability of statistical data or the testing method for the variables of each model;
- accuracy of the model when using the available data in relation to the required accuracy level.

For existing concrete structures a purely theoretical prediction by degradation modeling may be considerably improved in cases when some in–situ measurements of degradation effects are available (including results of health monitoring methods). Such "short–time" measurement results are statistically elaborated ("a priori information") and then utilized for Bayesian updating process; thus gaining "a posterior information". FReET provides such procedure. The description of this updating approach is also published in [11]. Considering the updated results of variables entering the limiting condition also the enhancement of reliability information may be gained.

2 CARBONATION OF CONCRETE

Concrete carbonation is chosen as a degradation process. It is a chemical process in concrete driven by ambient CO_2 penetrating from the surface and decreasing pH to a value approximately equal to 9. When the carbonation depth x_c equals the cover, a,

the steel is depassivated and corrosion may start (see also the initiation period explained above).

The process includes the diffusion of CO_2 in the gaseous phase into the concrete pores, its dissolution in the aqueous film of these pores, the dissolution of solid $Ca(OH)_2$ in the water of the pores, the diffusion of dissolved $Ca(OH)_2$ in pore water, its reaction with the dissolved CO_2, and the reaction of CO_2 with CSH (hydrated calcium silicate) and with the yet unhydrated C_3S (tricalcium silicate) and C_2S (dicalcium silicate). In addition, there is a parallel process. This process includes the hydration of cementitious materials and the reduction of concrete porosity.

The carbonation process indicates that the factors controlling carbonation are the diffusivity of CO_2 and the reactivity of CO_2 with concrete. The diffusivity of CO_2 depends upon the pore system of hardened concrete and the exposure condition. The pore system of concrete depends upon the type and the content of binder, the water/binder ratio, and the degree of hydration. The main exposure conditions related to the carbonation are the concentration of CO_2 and the relative humidity. The reactivity of CO_2 with concrete depends mainly upon the type and content of binder, and the degree of hydration. Thus, the main factors affecting concrete carbonation are the type and content of binder, the water/binder ratio, the degree of hydration, the concentration of CO_2, and the relative humidity. From this also follows: a general concrete property influencing carbonation rate is the pore structure. The rate of carbonation is also affected by the water and cement content, by the type of cement, the ground fineness of the materials, the temperature, curing and also by the alkali content and the presence of damaged zones and cracks.

2.1 Limit-state functions

Models concerning the carbonation of concrete can be utilized for evaluation of the limit-state equation (steel depassivation) in which the concrete cover, a, is compared to the carbonation depth, x_c, over time t - see also Eq. (10). As an alternative a critical initiation period t_i may be compared to design service life t_D. Please note, that in the following section introducing carbonation models only formulas for calculation of x_c are presented. An alternative output t_i may be derived by a simple inversion of individual equations. Note also that the uncertainty factor ψ which is used as a multiplier of output x_c is not inverted in any model thus the output time t_i is also multiplied by this factor.

2.2 Carbonation models

2.2.1 Carb1a

Formulae and input data

The model of the time-dependent carbonation depth x_c of OPC concrete developed by Papadakis et al. [13] is an analytical model based on the mass conservation of CO_2, $Ca(OH)_2$ and CSH in any control volume of a concrete mass. The simplified carbonation depth formula for OPC concrete is expressed here as:

$$x_c = \psi\, 0.35\, \rho_c \frac{\left(\frac{w}{c} - 0.3\right)}{\left(1 + \frac{\rho_c\, w}{1000\, c}\right)}\; f\,(RH) \sqrt{\left(1 + \frac{\rho_c\, w}{1000\, c} + \frac{\rho_c\, a_{1,2,3}}{\rho_a\, c}\right)\; C_{CO_2} \frac{24}{44}\; 10^{-6} t} \quad (11)$$

where x_c is the carbonation depth [mm] for time of exposure t [years], ρ_c, ρ_a are the specific gravities of cement and aggregates [kg/m^3], respectively, w, c, $a_{1,2,3}$ are the unit contents of water, cement and aggregates [kg/m^3], respectively, RH is the ambient relative humidity [%], C_{CO_2} is the CO_2 content in the atmosphere [mg/m^3] and ψ is the uncertainty factor of the model [-]. The unit contents of aggregates $a_{1,2,3}$ are calculated using the equation:

$$a_{1,2,3} = a_1 + a_2 + a_3 \tag{12}$$

where a_1, a_2, a_3 are the unit contents of aggregates I - III [kg/m^3]. Then, the specific gravity of the aggregates can be expressed as:

$$\rho_a = \frac{a_{1,2,3}}{\frac{a_1}{\rho_{a_1}} + \frac{a_2}{\rho_{a_2}} + \frac{a_3}{\rho_{a_3}}} \tag{13}$$

where ρ_{a_1}, ρ_{a_2}, ρ_{a_3} are the specific gravities of aggregates I - III [kg/m^3].

In its original form [13] the model was furnished by a linear function $f(RH)$ describing the influence of relative humidity RH (for $RH > 50\,\%$, maximum at $50\,\%$ - see Fig. 2 - dashed line), which does not provide satisfactory results for high values of RH according to some experimental findings. This has been overcome in the following model, *Carb1b*.

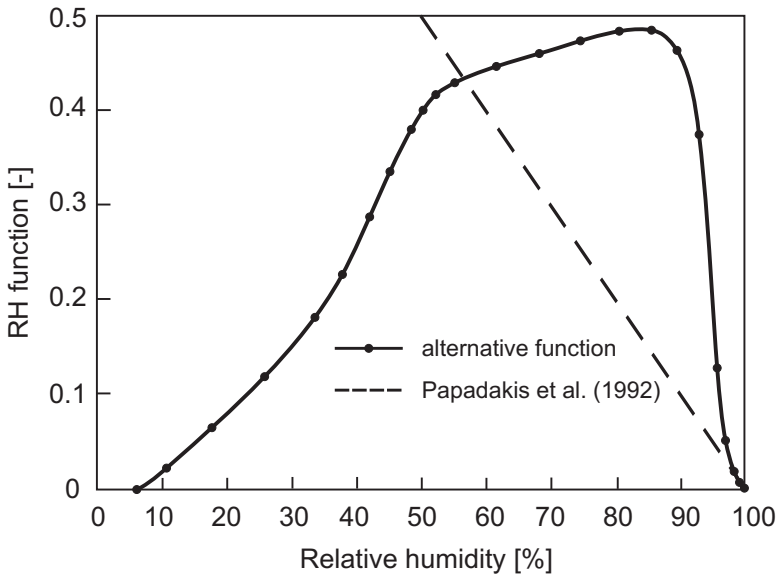

Figure 2: Two types of $f(RH)$ function.

2.2.2 Carb1b

Formulae and input data

To the authors best knowledge *Carb1a* does not provide satisfactory results for higher values of RH. This has been overcome by implementing the alternative function $f(RH)$ based on combination of experimental works - see Fig. 2, solid line. In this way the model *Carb1b* has been created which is similar to model *Carb1a*, i.e. Eqs. (11), (12) and (13).

Verification

A comparison of analytical results with the findings of tests carried out on an existing structure now follows: an RC cooling tower was investigated at the age of 19 years (the depth of carbonation was measured at 75 locations, both on internal and external surfaces) - for more details see [11]. Tab. 1 lists the results together with the analytical ones gained by *Carb1b*. The agreement is favorable, albeit the results of measurements being somewhat disqualified due to the well known inaccuracy of phenolphthalein tests.

Table 1: Carbonation depth after 19 years of exposure time

Surface	**Mean value [mm]**		**COV [%]**	
	measured	*model*	measured	*model*
External (RH= 70 %)	14.9	13.2	56	18
Internal (RH= 97 %)	8	8.2	29	18

3 INGRESS OF CHLORIDE IONS

Corrosion of reinforcement is certainly one of the most limiting factors for the service life of reinforced concrete structures. Steel bars are passive, as far as corrosion in the presence of oxygen and moisture is concerned, thanks to a microscopically thin oxide layer which forms on their surface due to the alkalinity of the surrounding concrete. This protective layer is dissolved if the alkalinity of the concrete is lost due to carbonation. However, in marine and coastal environments, or in the presence of deicing salt (NaCl), it can be destroyed by chloride ions dissolved in pore water.

The chloride level at the reinforcement surface which results in a significant corrosion rate leading to reinforcement corrosion in concrete may be called the critical chloride concentration (the chloride threshold concentration). Corrosion rates exceeding values of 1-2 μA/cm^2 are often regarded as being significant on reinforcing steel [7].

The chloride threshold concentration is preferably presented by means of the total amount of chloride by weight of cement, amount of a free chloride, a concentration ratio of free chloride ions to hydroxyl ions or ratio of acid soluble chloride content and the acid neutralization capacity (the content of acid needed to reduce the pH of concrete and cement paste suspended in water up to particular value) [1]. In terms of currently used representations, the total chloride content related to the cement weight is considered as the best alternative. This representation results in reduction in the range of determined values of the critical chloride concentration and represents the total potential aggressive ion content expressed relatively to the total potential inhibitor content [1, 4, 6, 7].

One reason for the lack of agreement among the measured values of the critical chloride concentration is the influence of several factors such as chloride binding, chloride mobility, steel interface (voidage, pre-rusting), cementitious binder (type of binder, C3A content, pH), concrete barrier (cement type, amount of cement, w/c ratio, curing, concrete cover), and environmental factors (relative humidity, temperature, chloride type). The key factor was found to be a physical condition of the steel-concrete interface [1, 6]. Another reason is

the difference among the methods of measurement of the chloride threshold concentration, the chloride content at the steel surface and the time of onset of corrosion. The onset of corrosion may be detected by measuring half-cell potential, monitoring the macrocell current between an anode and a cathode, monitoring the corrosion rate measured by the polarisation technique or AC impedance method, or visual inspection.

3.1 Limit-state functions

Models concerning the ingress of chloride ions can be utilized for evaluation of the limit-state equation (steel depassivation) in which the critical chloride concentration C_{cr} is compared to the actual chloride concentration $C(x = a, t)$ at depth a of the reinforcing steel at time t (models *Chlor2* and *Chlor3*), i.e. limit condition as Eq. (7). As an alternative a critical time to depassivation t_i is compared to design service life t_D (*Chlor1*), i.e. condition given by Eq. (2). *Chlor1* also allows for the computation of the depth of chlorination from the surface x_{Cl} in an arbitrary time, t.

3.2 Models for chloride ingress

Several different approaches exist for description of the time-dependent process of chloride ingress in concrete. Many authors have based their calculations on Fick's 2nd law of diffusion, taking into account the fact that observations indicate mainly diffusion controlled transport of chlorides in concrete, and the convection zone being relatively small [8], the Crank solution is often applied.

Although the models based on en error function complement solution are widely used by engineers in practical applications due to their relatively simple mathematical expressions, the ignorance of chloride binding is perhaps a weakness of these models. The models proposed by Papadakis et al. [15] differ from pure Fick's 2nd law just in the way that they also account for the processes of chloride adsorption and binding in the solid phase.

3.2.1 Chlor1a

Formulae and input data

A general model of the physicochemical processes of the diffusion-adsorption of chlorides in concrete has been developed by Papadakis et al. [15]. The model allows for prediction of the chloride concentration in the solid (s) and liquid (aq) phases of concrete ([Cl^-(s)] and [Cl^-(aq)] in mol/m^3 of concrete and mol/m^3 of pore water, respectively) as a function of the initial concentration of chlorides C_0, the concentration of chlorides on the nearest concrete surface $C_{S,0}$ [mol/m^3], their distance x [mm] from the nearest concrete surface, and time t [years]. The model can be simplified into a nonlinear differential equation for [Cl^-(aq)] and an algebraic one for [Cl^-(s)]:

$$\frac{\partial\,[Cl^-\,(aq)]}{\partial\,t} = \frac{\frac{D_{e,Cl^-}}{\varepsilon\,f}\;(1\,+\,\varepsilon\,f\,K_{eq}\;\,[Cl^-\,(aq)])^2}{K_{eq}\,C_{sat}\,+\,(1\,+\,\varepsilon\,f\,K_{eq}\;\,[Cl^-\,(aq)])^2}\;\,\frac{\partial^2\,[Cl^-\,(aq)]}{\partial x^2} \tag{14}$$

$$[Cl^-(s)] = \frac{\varepsilon\,f\,K_{eq}\,C_{sat}\;[Cl^-\,(aq)]}{1\,+\,\varepsilon\,f\,K_{eq}\;\,[Cl^-\,(aq)]} \tag{15}$$

with the initial condition: $[Cl^-(aq)] = C_0$ at $t = 0$, and boundary conditions $[Cl^-(aq)] = C_{S,0}$ at $x = 0$ and $[Cl^-(aq)]/\partial x = 0$. In these equations D_{e,Cl^-} denotes the effective diffusivity of Cl^- in concrete [m^2/s], K_{eq} the equilibrium constant for Cl^- binding [m^3 of concrete/mol], C_{sat} the saturation concentration of Cl^- in the solid phase [m^3 of concrete/mol], ε the concrete porosity and f the degree of pore saturation with water.

Eq. (14) can be solved only numerically. A simple analytical approximation can be developed, if we make the assumption of the formation of a moving "chlorination front", where the concentration of $[Cl^-(aq)]$ decreases to zero. Then, the concentration of Cl^- in the liquid phase of concrete decreases linearly from $C_{S,0}$ on the nearest surface to zero at the chlorination front. The distance from the nearest surface to the chlorination front (the depth of chlorination x_{Cl} [mm]) is given by the following expression:

$$x_{Cl} = \psi\, 1000 \sqrt{\frac{3.1536 \cdot 2D_{e,Cl^-} \cdot C_{S,0}}{C_{sat}} t \cdot 10^7} \tag{16}$$

where ψ is the uncertainty factor of the model [-], other symbols have the same descriptions and units as in Eqs. (14) and (15). In fully saturated and fully hydrated OPC concrete, the effective diffusivity D_{e,Cl^-} is given by the following semi-empirical expression:

$$D_{e,Cl^-} = 0.15 \frac{1 + \frac{\rho_c}{1000}\frac{w}{c}}{1 + \frac{\rho_c}{1000}\frac{w}{c} + \frac{\rho_c}{\rho_a} \cdot \frac{a_{1,2,3}}{c}} \left[\frac{\frac{\rho_c}{1000}\frac{w}{c} - 0.85}{1 + \frac{\rho_c}{1000}\frac{w}{c}} \right]^3 D_{Cl^-,H_2O} \tag{17}$$

where D_{Cl^-,H_2O} denotes the diffusion coefficient of Cl^- in an "infinite solution" [m^2/s] ($1.6 \cdot 10^{-9}$ m^2/s and $1.3 \cdot 10^{-9}$ m^2/s in the case of NaCl and $CaCl_2$, respectively), ρ_c and ρ_a (see Eq. (13)) are the specific gravities of cement and aggregate [kg/m^3], respectively, and w, c and $a_{1,2,3}$ (see Eq. (12)) represent the unit contents of water, cement and aggregates [kg/m^3], respectively.

If C_{cr} indicates the threshold concentration of Cl^- in the aqueous phase [mol/m^3] required for the depassivation of steel bars (13.4 mol/m^3 in the case of NaCl), a is the concrete cover [mm] and ψ is the uncertainty factor of the model [-], then time t_i [years] to depassivation is given by:

$$t_i = \psi \frac{C_{sat}\,(a/1000)^2}{3.1536 \cdot 10^7 \cdot 2D_{e,Cl^-} \cdot C_{S,0} \left(1 - \frac{C_{cr}}{C_{S,0}}\right)^2} \tag{18}$$

The saturation concentration of Cl^- in the solid phase C_{sat} can be determined from the slope of the straight lines fitted to the test data on the steady-state values of $[Cl^-(aq)]$ and $[Cl^-(s)]$ in concrete samples with known initial concentrations C_0, see [14, 16].

4 EXAMPLES

4.1 Example 1 – General utilization of FReET-D (*Carb1b*)

An elementary example of FReET-D utilization is shown in this section. The goal of the analysis is to predict a depth of carbonated concrete layer after 50 years of service life, using a simple carbonation model. Typical progress of analysis processing is introduced in subsequent steps corresponding to key entries of the main program tree. Details to each step of an analysis performed using the software FReET can be found in FReET Program Documentation – Part 2 – FReET M/A User Manual [12].

Random Variables: After initialization of the program FReET, the template *carb.fre* file is opened from certain location of user's hard drive, where the FReET-D files have been copied. After file opening, the program proceeds to the Part "Stochastic Model", Item "Random Variables" of the Main Programme Tree (MPT), on a sheet corresponding to first category of random variables (in this case the category sheet of models ***Carb1a Carb1b***), as shown in Fig. 3.

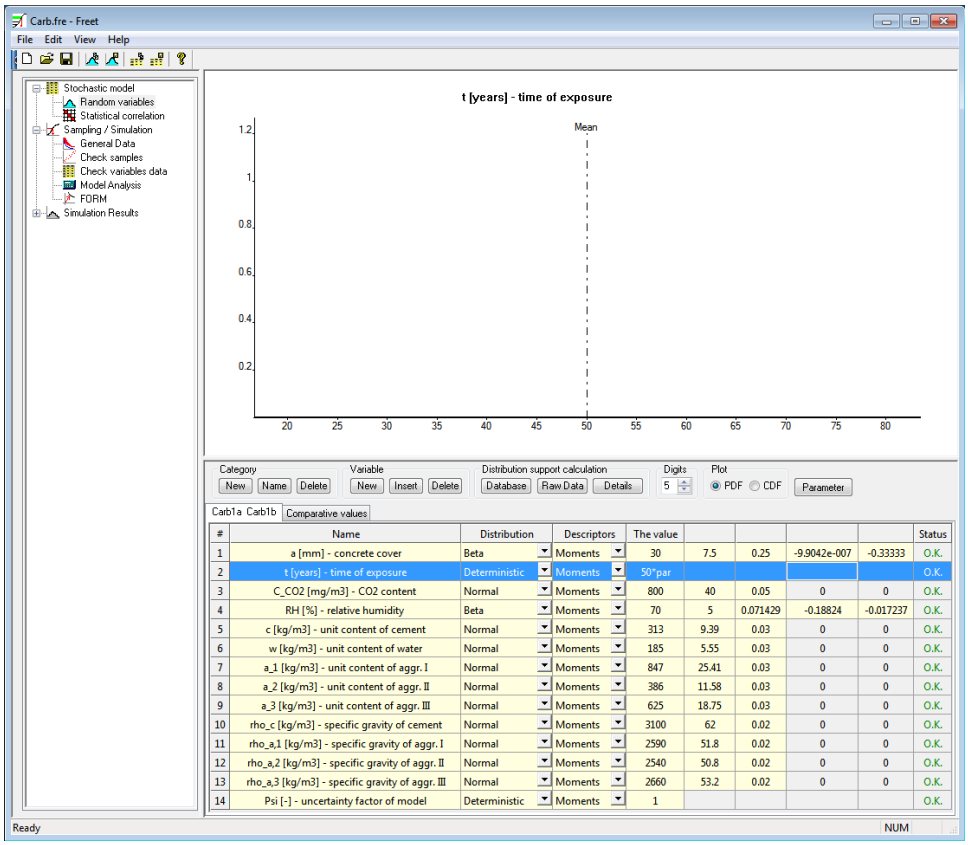

Figure 3: Opening of template *carb.fre* file

Values of input variables can be changed on this sheet. In presented example, the input values as well as their distributions are kept default within this example.

We are interested in the progress of carbonation in time. Therefore the input variable time t [years] is multiplied by a parameter defined as a set of values from 0.2 to 2 with step 0.2, as shown in Fig. 4. In this way the analysis will be performed for times 10, 20, ..., 50, ..., 100 years.

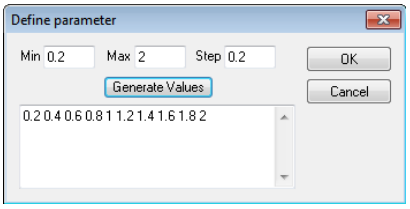

Figure 4: Definition of parameter

Statistical Correlation: Statistical correlation among input random variables could be imposed in the window appearing after double-clicking on Item "Statistical Correlation" within Part "Stochastic Model" of MPT. In the case of the model ***Carb1b*** the correlation of input variables would not be real. Therefore it is not shown here; details concerning the statistical correlation can be found in FReET Program Documentation – Part 2 – FReET M/A User Manual [12].

General Data: Simulation of random variables is run in the window appearing after double-clicking on Item "General Data" in Part "Sampling / Simulation" of MPT. The number of simulations is set to 1000 for this analysis. The real simulation is launched by clicking on the "Run" button. Random input parameters are generated according to their PDFs using Monte Carlo type simulation and samples are reordered by simulated annealing approach in order to match required correlation matrix as close as possible. The information about achieved accuracy is displayed after simulated annealing process, as shown in Fig. 5. For more information see FReET Program Documentation – Part 2 – FReET M/A User Manual [12].

Check Samples: The generated random realization of input random variables can be checked under Item "Check Samples" of MPT on category sheet ***Carb1a Carb1b***. When user clicks outside of diagonal of the correlation matrix displayed in the table part of main graphic display, the upper graphical part shows the image of sampled values in Cartesian, as shown in Fig. 6.

Check Variables Data: Individual values of sampled realizations of each input random variable can be examined in the table in the lower part of main graphic display. The table can be enlarged by dragging its upper edge for more convenient treatment, as shown in Fig. 7. If needed, the values can be easily exported from this table simply by copying and pasting to a spreadsheet program (e.g. MS Excel).

Model Analysis: The window "Model Analysis" appears after double-clicking on the fourth item of Part "Sampling / Simulation" of MPT. Clicking on the button "New Model Function" adds new row in the table in the lower part of the main program

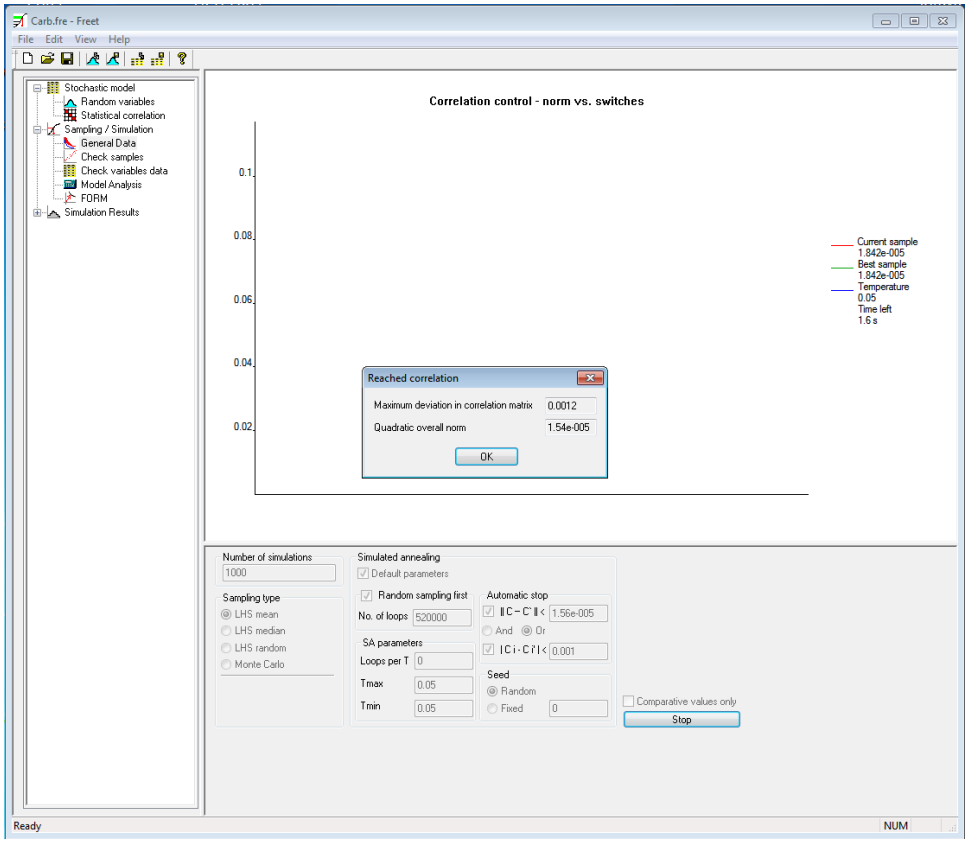

Figure 5: Sampling of random variables and statistical correlation imposing by simulated annealing approach

window. By clicking on "..." button in this row, FReET will open a browse window to input a file with DLL function which contains desired model function(s), in this case *carb1b.dll*, as shown in Fig. 8. The *carb1b_xc* option is to be chosen from the two available ones offered in the pull-down menu in the column "Exported functions" (see Fig. 9). The default result name *Xlimit 1* in the last column of the table can be renamed to x_c *[mm] – carbonation depth*, as the carbonation depth is the selected output of the model function programmed in *carb1b.dll*. The model analysis is started by button "Run Model Analysis".

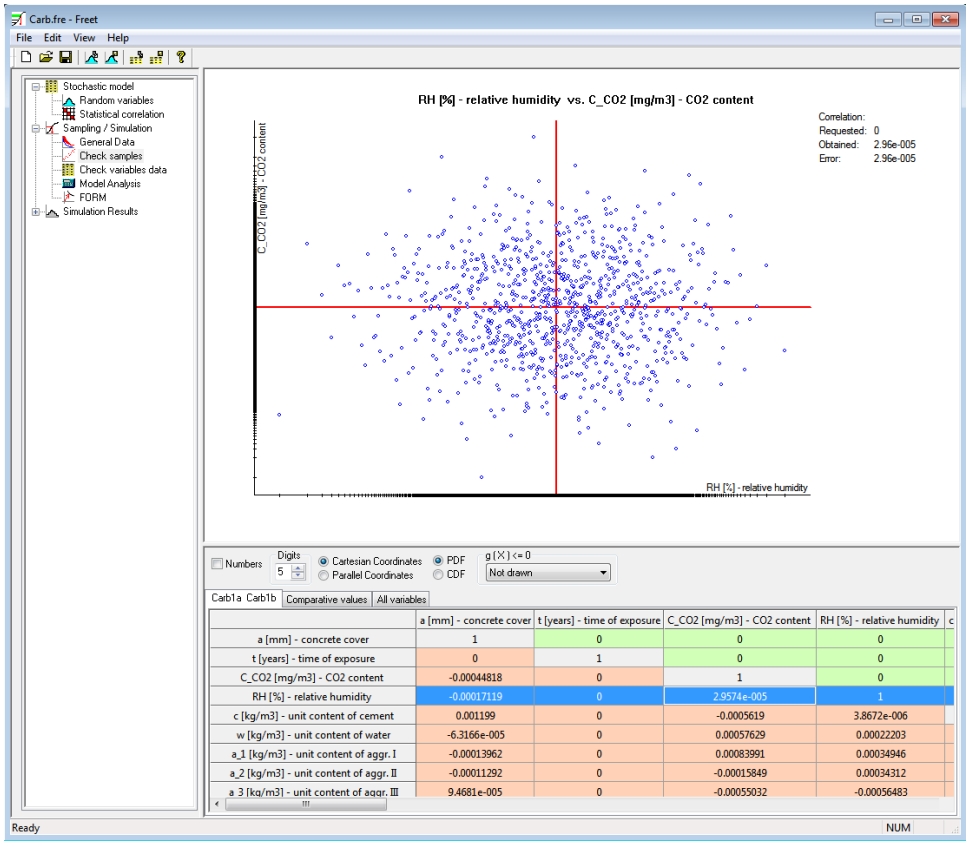

	a [mm] - concrete cover	t [years] - time of exposure	C_CO2 [mg/m3] - CO2 content	RH [%] - relative humidity
a [mm] - concrete cover	1	0	0	0
t [years] - time of exposure	0	1	0	0
C_CO2 [mg/m3] - CO2 content	-0.00044818	0	1	0
RH [%] - relative humidity	-0.00017119	0	2.9574e-005	1
c [kg/m3] - unit content of cement	0.001199	0	-0.0005619	3.8672e-006
w [kg/m3] - unit content of water	-6.3166e-005	0	0.00057629	0.00022203
a_1 [kg/m3] - unit content of aggr. I	-0.00013962	0	0.00083991	0.00034946
a_2 [kg/m3] - unit content of aggr. II	-0.00011292	0	-0.00015849	0.00034312
a_3 [kg/m3] - unit content of aggr. III	9.4681e-005	0	-0.00055032	-0.00056483

Figure 6: Sampled values of random variables in Cartesian coordinates

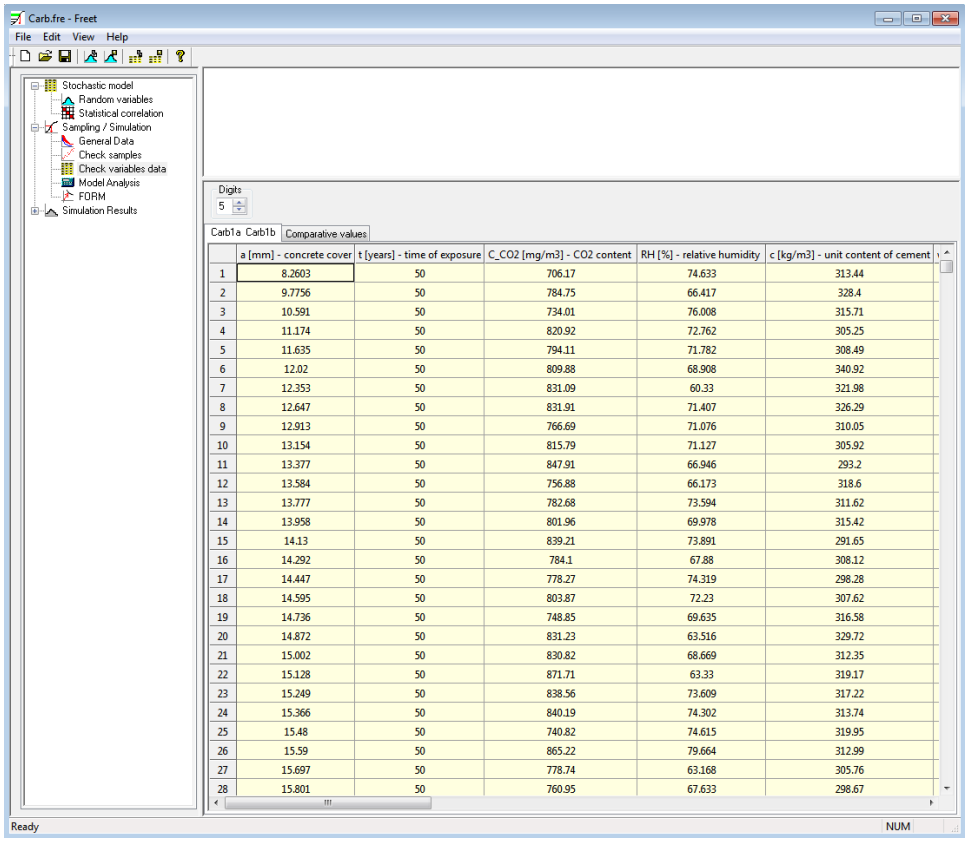

	a [mm] - concrete cover	t [years] - time of exposure	C_CO2 [mg/m3] - CO2 content	RH [%] - relative humidity	c [kg/m3] - unit content of cement
1	8.2603	50	706.17	74.633	313.44
2	9.7756	50	784.75	66.417	328.4
3	10.591	50	734.01	76.008	315.71
4	11.174	50	820.92	72.762	305.25
5	11.635	50	794.11	71.782	308.49
6	12.02	50	809.88	68.908	340.92
7	12.353	50	831.09	60.33	321.98
8	12.647	50	831.91	71.407	326.29
9	12.913	50	766.69	71.076	310.05
10	13.154	50	815.79	71.127	305.92
11	13.377	50	847.91	66.946	293.2
12	13.584	50	756.88	66.173	318.6
13	13.777	50	782.68	73.594	311.62
14	13.958	50	801.96	69.978	315.42
15	14.13	50	839.21	73.891	291.65
16	14.292	50	784.1	67.88	308.12
17	14.447	50	778.27	74.319	298.28
18	14.595	50	803.87	72.23	307.62
19	14.736	50	748.85	69.635	316.58
20	14.872	50	831.23	63.516	329.72
21	15.002	50	830.82	68.669	312.35
22	15.128	50	871.71	63.33	319.17
23	15.249	50	838.56	73.609	317.22
24	15.366	50	840.19	74.302	313.74
25	15.48	50	740.82	74.615	319.95
26	15.59	50	865.22	79.664	312.99
27	15.697	50	778.74	63.168	305.76
28	15.801	50	760.95	67.633	298.67

Figure 7: Sampled values of random variables

The user should verify, if a text file *err_carb1b.txt* has been generated to a directory, from which the *carb1b.dll* file was loaded for the model analysis. A message e.g. '2. variable "CO2 content in the atmosphere" is not correct (cannot be negative)' may occur several times in the error file. In such a case it is recommended to change the type of distribution of the indicated input variable (e.g. CO_2 content in the atmosphere) to other appropriate one to avoid the simulation of unreal values (for CO_2 content in the atmosphere e.g. OneBounded Normal distribution with unchanged *Mean* and *Std* and *bound* set to 0 can be suitable).

Histograms: The distribution of output of the model analysis is displayed in the window "Histograms" of Part "Simulation Results" of MPT. The distribution of the output random variable corresponding to a time point appropriate to a particular value of the parameter selected in the combo box "Parameter" is displayed. Probability distribution function of the carbonation depth at time $t = 50$ years (for value of parameter equal to 1) with relevant distribution details, is shown in Fig. 10.

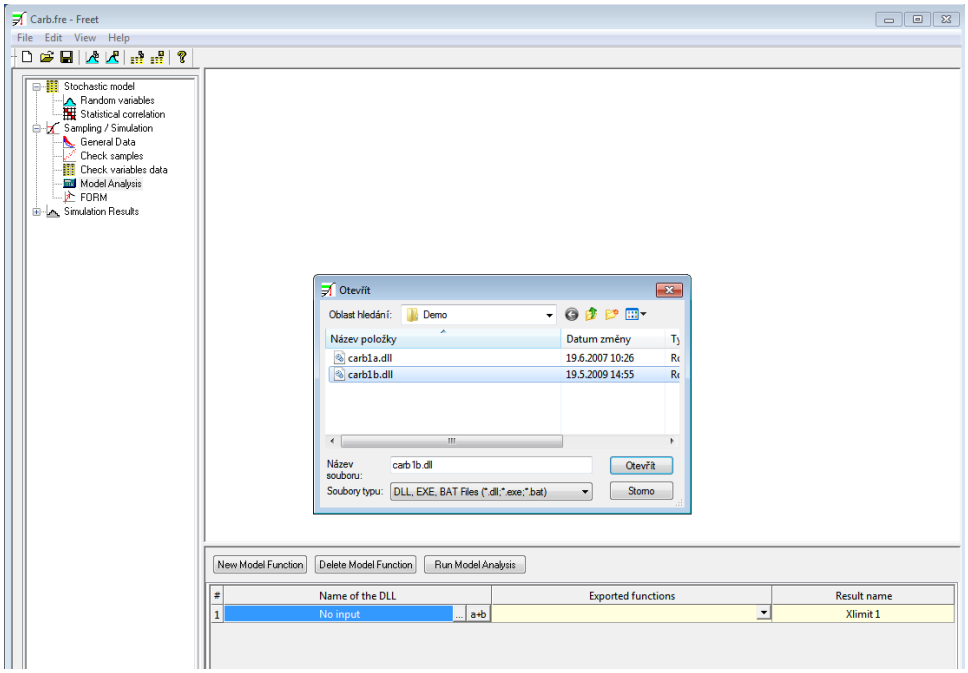

Figure 8: Loading of *carb1b.dll* file with defined model function for model analysis

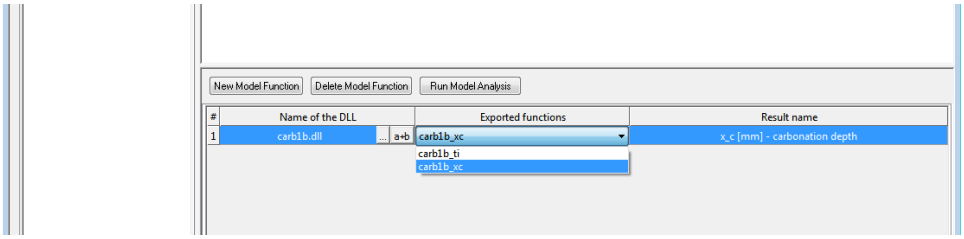

Figure 9: Selecting the appropriate model function for carbonation depth analysis

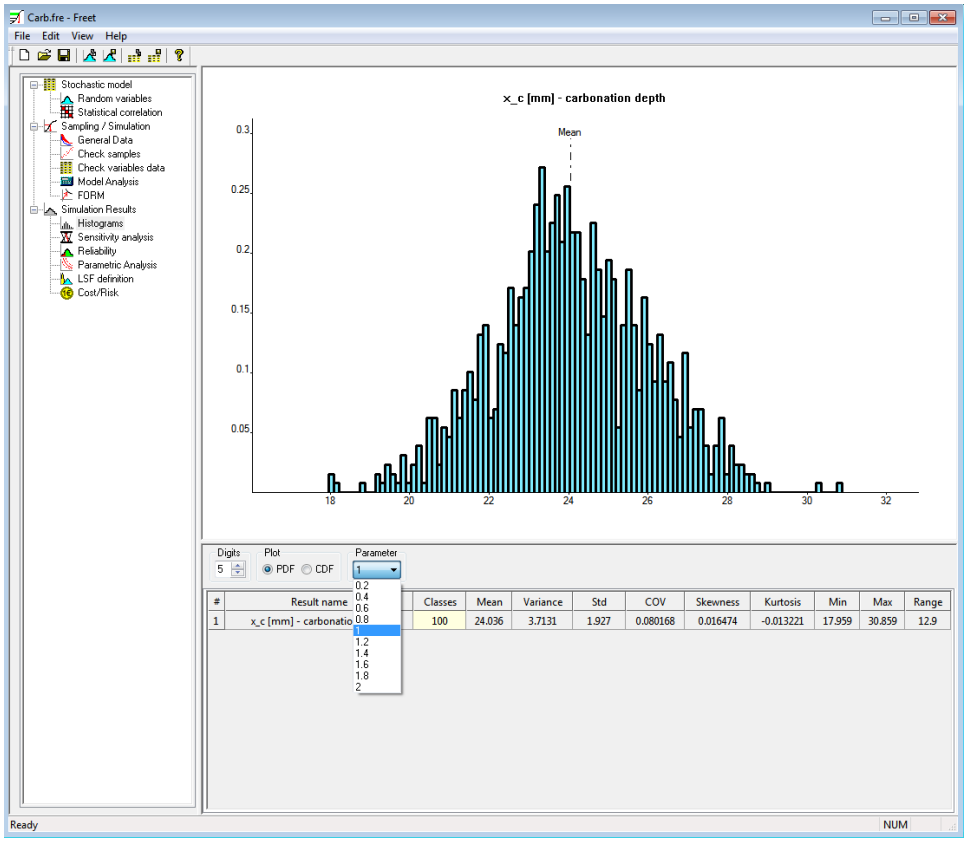

Figure 10: PDF of carbonation depth in $t = 50$ years

LSF Definition: The entry "LSF Definition" of Part "Simulation Results" of MPT enables user to define limit state function for sensitivity and reliability analysis. After clicking on the button "New LSF" a new row appears in the table part of the main graphic display, where the limit state function is defined as a combination of output of the model analysis and appropriate comparative value. In presented example, the limit state function is defined as a difference between concrete cover a [mm] and carbonation depth x_c [mm], as shown in Fig. 11. Default comparative value included in the template file *carb.fre* is used for the definition in this case.

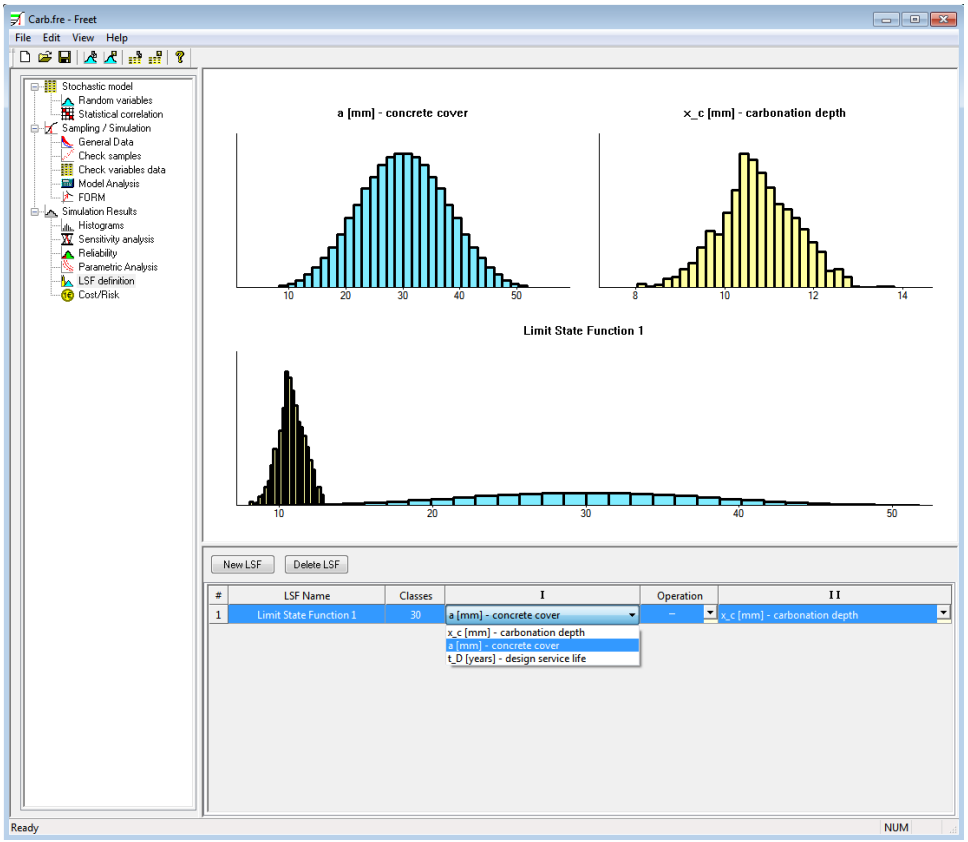

Figure 11: Definition of limit state function

Sensitivity Analysis: Item "Sensitivity Analysis" of MPT opens a window, where sensitivity of input parameters is evaluated. Factors in columns "+sensi" and "−sensi" represent the sensitivity of the inputs of individual deterioration models on results of model analysis or defined limit state functions. In this case only parameters appropriate to models ***Carb1a Carb1b*** are relevant, as emphasized in Fig. 12. The time point of the analysis can be changed using the combo box "Parameter". Detailed description of Item "Sensitivity Analysis" of MPT is included in FReET Program Documentation – Part 2 – FReET M/A User Manual [12].

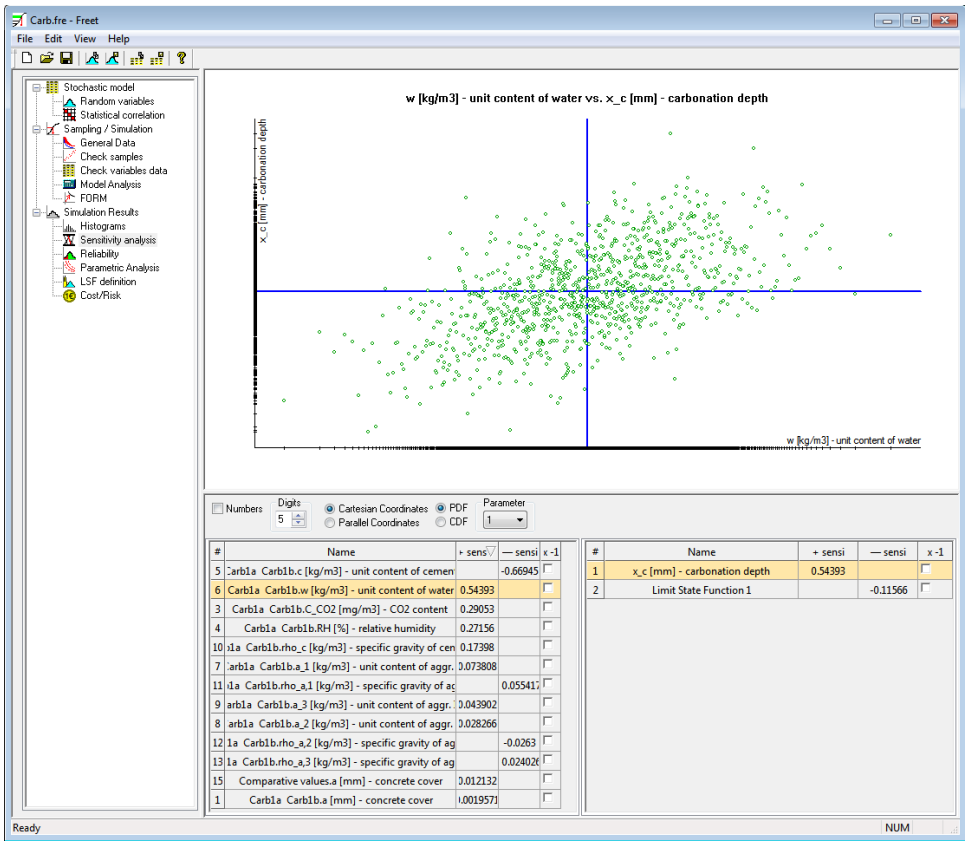

Figure 12: Sensitivity of input parameters on the carbonation depth

Reliability: The entry "Reliability" of Part "Simulation Results" of MPT opens a window for reliability assessment of performed analysis. If a particular value of the parameter is entered by the combo box "Parameter", the distributions of output of model analysis or defined limit state function is displayed in the main graphic display. Fig. 13 shows the PDF of defined limit state function at time $t = 50$ years (value of parameter is equal to 1). Let us note, that the reliability parameters Cornell-β and corresponding p_f can be alternatively to the LHS method, applied in this case, obtained by using the FORM method under the item "FORM" of MPT, moreover, the latter method leads to more accurate results. Comparison of the reliability parameters obtained via LHS and FORM can be made in Fig. 13 and Fig. 14, respectively.

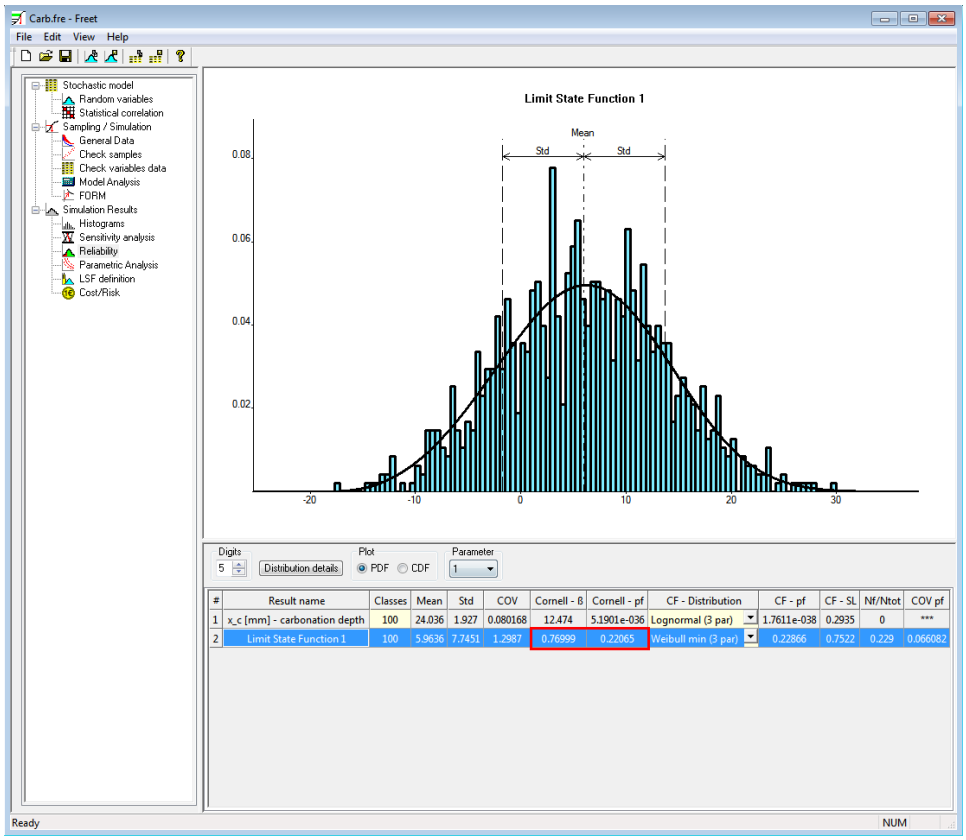

Figure 13: PDF of defined limit state function at time $t = 50$ years

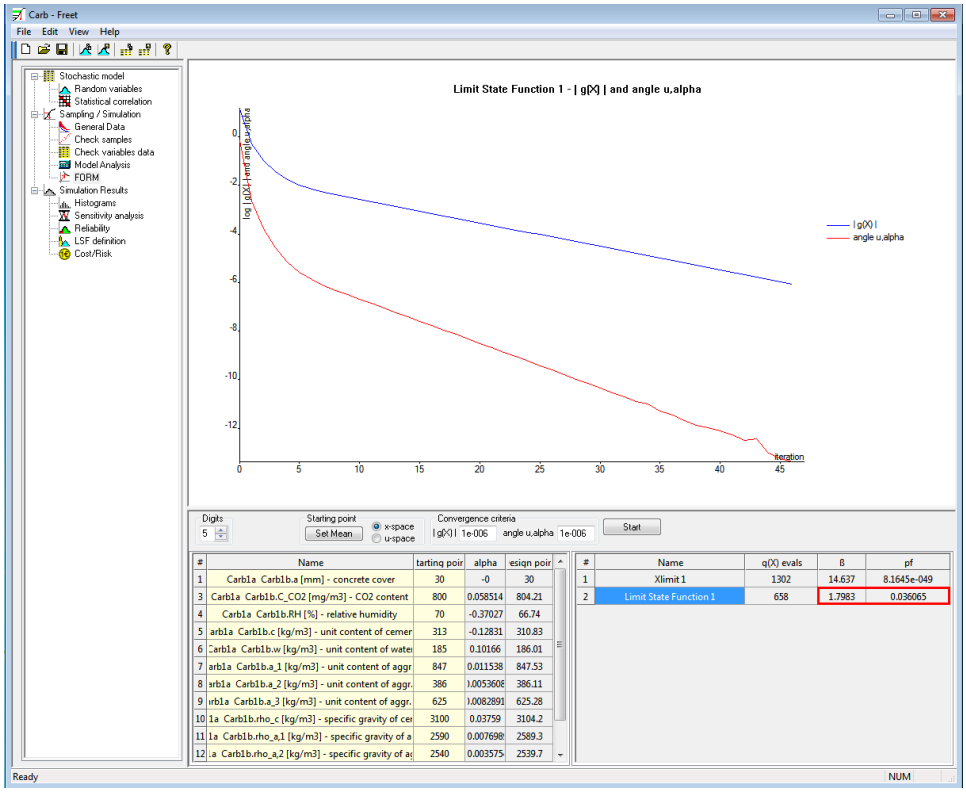

Figure 14: Reliability analysis using FORM method at time $t = 50$ years

Parametric Analysis: Time series of statistical and reliability parameters of outputs of model analysis or limit state functions can be displayed under this item of MPT. If the output of model analysis is chosen in the combo box "Result & LSF" (the carbonation depth x_c [mm] in this case), a curve of $Mean$ (mean value) and $Mean \pm Std$ (Std stands for standard deviation) of the output random variable as a function of parameterized input variable (time t in this case) is drawn in the graphical part of the main window, as shown in Fig. 15. The table part lists statistical and reliability parameters of the output variable for each defined value of the parameter (in each time step from 10 to 100 years in this case). The display stay unchanged, when clicking in the statistical section of the table part of the main window (8 columns from "Mean" to "Range") for any value of the parameter. When the click is targeted to the reliability section (columns presenting Cornell's reliability index Cornell-β, corresponding failure probability p_f, the failure probability estimation based on curve fitting CF-p_f, and the failure probability estimation based on classical frequency definition of probability N_f/N_{tot}), nothing is displayed in the main graphical window in this case as these parameters lack sense for the model function in this type of analysis.

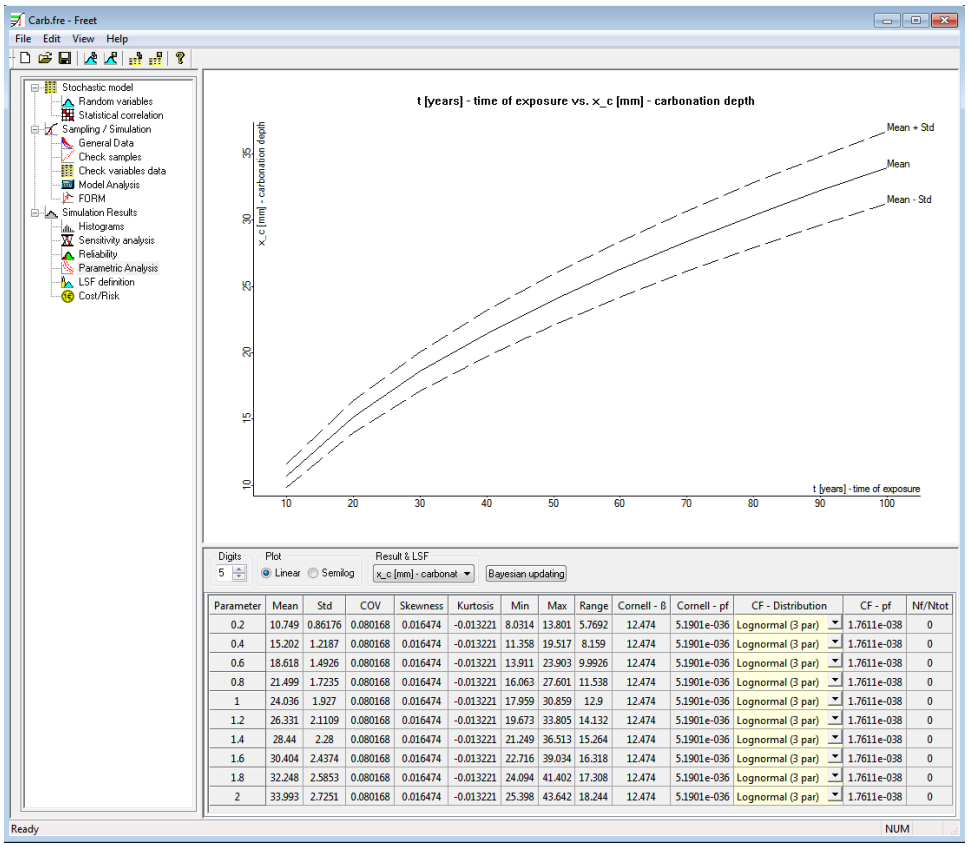

Parameter	Mean	Std	COV	Skewness	Kurtosis	Min	Max	Range	Cornell - ß	Cornell - pf	CF - Distribution	CF - pf	Nf/Ntot
0.2	10.749	0.86176	0.080168	0.016474	-0.013221	8.0314	13.801	5.7692	12.474	5.1901e-036	Lognormal (3 par)	1.7611e-038	0
0.4	15.202	1.2187	0.080168	0.016474	-0.013221	11.358	19.517	8.159	12.474	5.1901e-036	Lognormal (3 par)	1.7611e-038	0
0.6	18.618	1.4926	0.080168	0.016474	-0.013221	13.911	23.903	9.9926	12.474	5.1901e-036	Lognormal (3 par)	1.7611e-038	0
0.8	21.499	1.7235	0.080168	0.016474	-0.013221	16.063	27.601	11.538	12.474	5.1901e-036	Lognormal (3 par)	1.7611e-038	0
1	24.036	1.927	0.080168	0.016474	-0.013221	17.959	30.859	12.9	12.474	5.1901e-036	Lognormal (3 par)	1.7611e-038	0
1.2	26.331	2.1109	0.080168	0.016474	-0.013221	19.673	33.805	14.132	12.474	5.1901e-036	Lognormal (3 par)	1.7611e-038	0
1.4	28.44	2.28	0.080168	0.016474	-0.013221	21.249	36.513	15.264	12.474	5.1901e-036	Lognormal (3 par)	1.7611e-038	0
1.6	30.404	2.4374	0.080168	0.016474	-0.013221	22.716	39.034	16.318	12.474	5.1901e-036	Lognormal (3 par)	1.7611e-038	0
1.8	32.248	2.5853	0.080168	0.016474	-0.013221	24.094	41.402	17.308	12.474	5.1901e-036	Lognormal (3 par)	1.7611e-038	0
2	33.993	2.7251	0.080168	0.016474	-0.013221	25.398	43.642	18.244	12.474	5.1901e-036	Lognormal (3 par)	1.7611e-038	0

Figure 15: Time series of $Mean$ value and $Mean \pm Std$ value of carbonation depth

If the defined limit state function is chosen in the combo box “Result & LSF”, a time dependence of $Mean$ and $Mean \pm Std$ of this LSF is displayed in the main graphical window, as shown in Fig. 16. When clicking in the reliability section of the table part of the main window, a time dependence of the reliability parameter appropriate to the selected column is drawn in the main graphic window. Time series of Cornell-β defined within presented example is shown in Fig. 17.

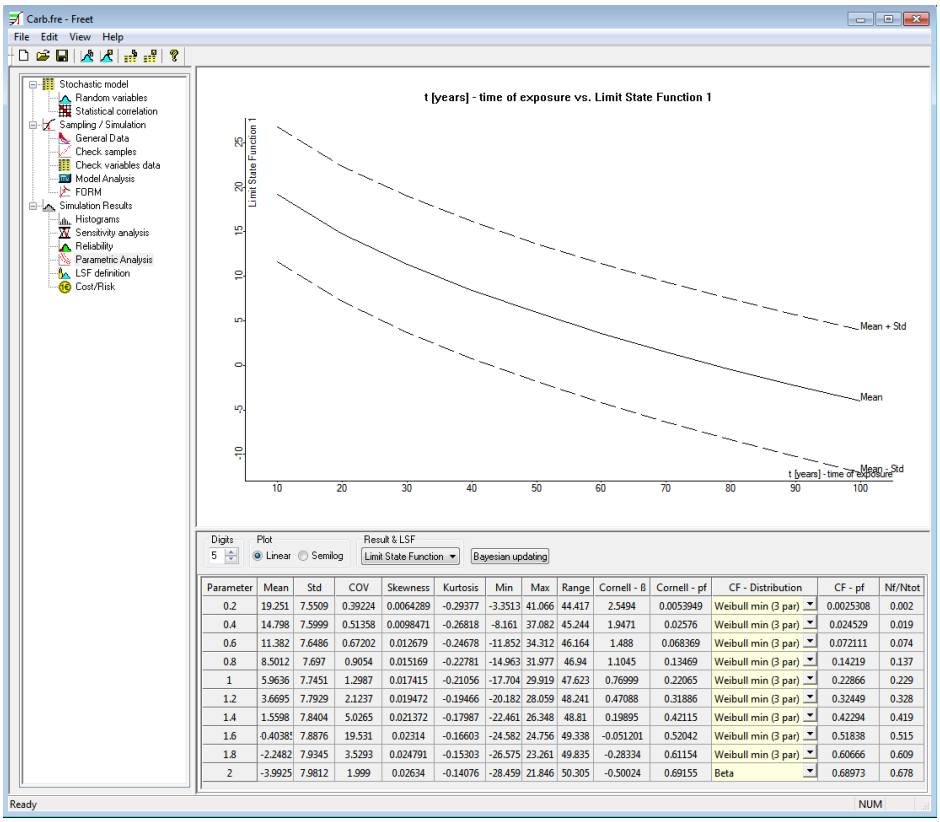

Parameter	Mean	Std	COV	Skewness	Kurtosis	Min	Max	Range	Cornell - ß	Cornell - pf	CF - Distribution	CF - pf	Nf/Ntot
0.2	19.251	7.5509	0.39224	0.0064289	-0.29377	-3.3513	41.066	44.417	2.5494	0.0053949	Weibull min (3 par)	0.0025308	0.002
0.4	14.798	7.5999	0.51358	0.0098471	-0.26818	-8.161	37.082	45.244	1.9471	0.02576	Weibull min (3 par)	0.024529	0.019
0.6	11.382	7.6486	0.67202	0.012679	-0.24678	-11.852	34.312	46.164	1.488	0.068369	Weibull min (3 par)	0.072111	0.074
0.8	8.5012	7.697	0.9054	0.015169	-0.22781	-14.963	31.977	46.94	1.1045	0.13469	Weibull min (3 par)	0.14219	0.137
1	5.9636	7.7451	1.2987	0.017415	-0.21056	-17.704	29.919	47.623	0.76999	0.22065	Weibull min (3 par)	0.22866	0.229
1.2	3.6695	7.7929	2.1237	0.019472	-0.19466	-20.182	28.059	48.241	0.47088	0.31886	Weibull min (3 par)	0.32449	0.328
1.4	1.5598	7.8404	5.0265	0.021372	-0.17987	-22.461	26.348	48.81	0.19895	0.42115	Weibull min (3 par)	0.42294	0.419
1.6	-0.40385	7.8876	19.531	0.02314	-0.16603	-24.582	24.756	49.338	-0.051201	0.52042	Weibull min (3 par)	0.51838	0.515
1.8	-2.2482	7.9345	3.5293	0.024791	-0.15303	-26.575	23.261	49.835	-0.28334	0.61154	Weibull min (3 par)	0.60666	0.609
2	-3.9925	7.9812	1.999	0.02634	-0.14076	-28.459	21.846	50.305	-0.50024	0.69155	Beta	0.68973	0.678

Figure 16: Time series of $Mean$ value and $Mean \pm Std$ value of defined limit state function

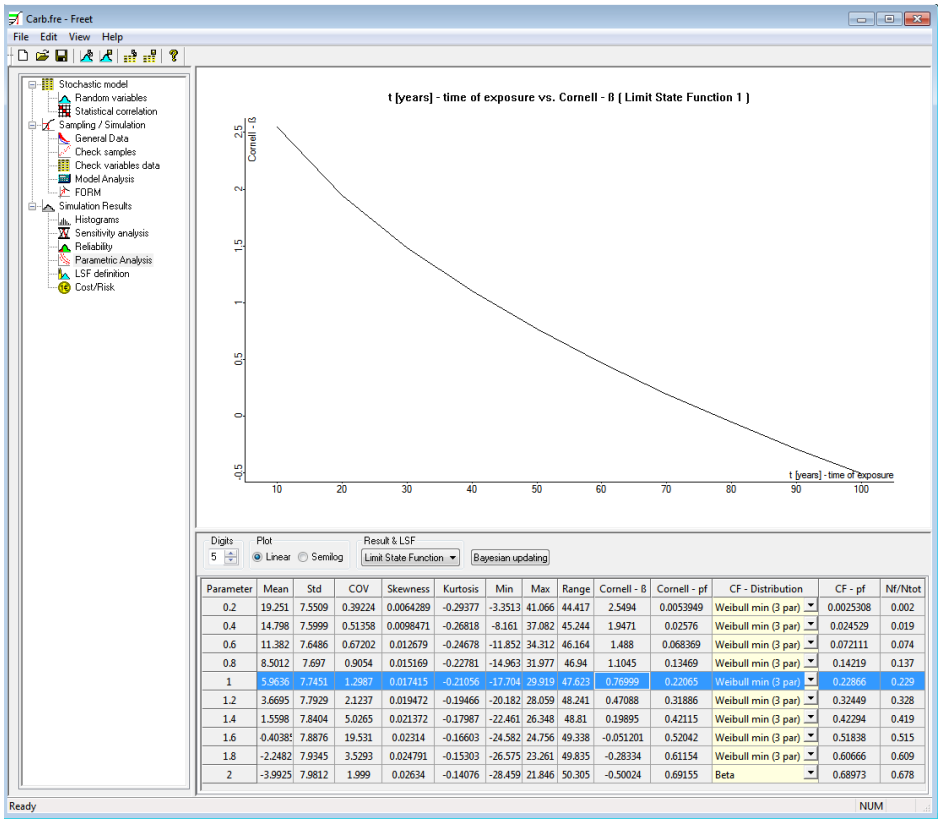

Parameter	Mean	Std	COV	Skewness	Kurtosis	Min	Max	Range	Cornell - ß	Cornell - pf	CF - Distribution	CF - pf	Nf/Ntot
0.2	19.251	7.5509	0.39224	0.0064289	-0.29377	-3.3513	41.066	44.417	2.5494	0.0053949	Weibull min (3 par)	0.0025308	0.002
0.4	14.798	7.5999	0.51358	0.0098471	-0.26818	-8.161	37.082	45.244	1.9471	0.02576	Weibull min (3 par)	0.024529	0.019
0.6	11.382	7.6486	0.67202	0.012679	-0.24678	-11.852	34.312	46.164	1.488	0.068369	Weibull min (3 par)	0.072111	0.074
0.8	8.5012	7.697	0.9054	0.015169	-0.22781	-14.963	31.977	46.94	1.1045	0.13469	Weibull min (3 par)	0.14219	0.137
1	5.9636	7.7451	1.2987	0.017415	-0.21056	-17.704	29.919	47.623	0.76999	0.22065	Weibull min (3 par)	0.22866	0.229
1.2	3.6695	7.7929	2.1237	0.019472	-0.19466	-20.182	28.059	48.241	0.47088	0.31886	Weibull min (3 par)	0.32449	0.328
1.4	1.5598	7.8404	5.0265	0.021372	-0.17987	-22.461	26.348	48.81	0.19895	0.42115	Weibull min (3 par)	0.42294	0.419
1.6	0.40385	7.8876	19.531	0.02314	-0.16603	-24.582	24.756	49.338	-0.051201	0.52042	Weibull min (3 par)	0.51838	0.515
1.8	-2.2482	7.9345	3.5293	0.024791	-0.15303	-26.575	23.261	49.835	-0.28334	0.61154	Weibull min (3 par)	0.60666	0.609
2	-3.9925	7.9812	1.999	0.02634	-0.14076	-28.459	21.846	50.305	-0.50024	0.69155	Beta	0.68973	0.678

Figure 17: Time series of Cornell's reliability index Cornell-β for defined limit state function

4.2 Example 2 – Time to reinforcement depassivation (*Carb1b*, *Chlor1a*)

This example illustrates the calculation of time to reinforcement depassivation t_i (initiation time) due to carbonation and/or chloride ingress dependent on the concrete cover thickness a (this quantity being assumed here in the range from 25 to 75 mm). The full description of all input values is given in Tab. 8.

Reflection of	**Variable**	**Unit**	***Mean***	***COV***	**PDF**
Models	uncertainty factor of model	-	1	0.15	Lognormal (2par)
Environment	CO_2 content in the atmosphere	mg/m^3	820	0.12	Normal
	relative humidity	%	70	0.07	Beta (a = 0, b = 100)
	concentration of Cl^- on nearest concrete surface	mol/m^3	50	-	Deterministic
Concrete mix	unit content of OPC cement	kg/m^3	313	0.03	Normal
	unit content of water	kg/m^3	185	0.03	Normal
	unit content of aggregate (0–4 mm)	kg/m^3	847	0.03	Normal
	unit content of aggregate (4–8 mm)	kg/m^3	386	0.03	Normal
	unit content of aggregate (8–16 mm)	kg/m^3	625	0.03	Normal
	specific gravity of cement	kg/m^3	3100	0.02	Normal
	specific gravity of aggregate (0–4 mm)	kg/m^3	2590	0.02	Normal
	specific gravity of aggregate (4–8 mm)	kg/m^3	2540	0.02	Normal
	specific gravity of aggregate (8–16 mm)	kg/m^3	2660	0.02	Normal
Other	concrete cover	mm	25–75	-	Deterministic
	saturation concentration of Cl^- in solid phase	mol/m^3	140	-	Deterministic
	threshold concentration of Cl^- in liquid phase	mol/m^3	13.4	-	Deterministic
	diffusion coefficient of Cl^- in infinite solution	m^2/s	1.6e-9	-	Deterministic

Table 2: Input parameters for the calculation of time to reinforcement depassivation (models ***Carb1b*** and ***Chlor1a***)

Let us comment here the most important ones. For carbonation it is the CO_2 content in the atmosphere (Normal distribution, $Mean = 820$, $Std = 98.4$) [mg/m^3] and the relative humidity RH (Beta distribution, $Mean = 70$, $a = 0$, $b = 100$) [%]. For chloride ingress it is the concentration of chlorides (de-icing salts) on the concrete surface $C_{S,0}$ assumed by the deterministic value of 50 [mol/m^3] and the critical concentration of Cl in pore solution

C_{cr} taken by the deterministic value of 13.4 [mol/m^3]. The results of performed statistical analysis are shown in Fig. 18, where mean values together with standard deviations are plotted. Let us focus on a concrete cover $a = 45$ mm and apply following conditions:

$$P_f(t_D) = P\left\{a - x_c(t_D) \leq 0\right\} \leq P_d \ , \tag{19}$$

$$P_f(t_D) = P\left\{C_{cr} - C_a(t_D) \leq 0\right\} \leq P_d \ , \tag{20}$$

where t_D is the target design life of considered value 50 years. We obtain $\beta = 2.85$ ($P_f = 2 \times 10^3$) and $\beta = 0.7$ ($P_f = 2 \times 10^1$, not an acceptable value) for depassivation due to carbonation and chloride ingress, respectively. The well known fact that the rate of chloride ingress is greater compared to the carbonation rate with respect to time to depassivation is also evident from this example. The best probability density function (PDF) fitted for resulting times is Lognormal (2par).

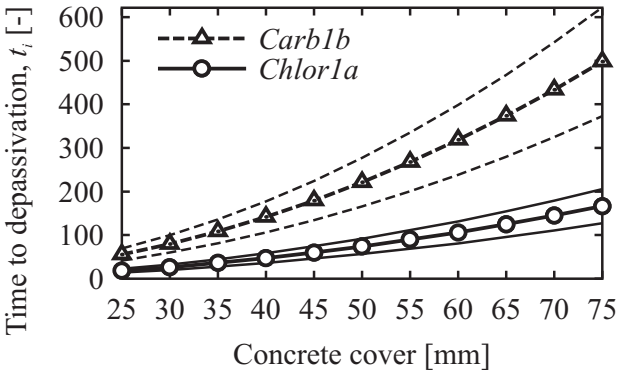

Figure 18: Time to depassivation (mean value ± standard deviation) due to carbonation and chloride ingress vs. concrete cover

References

[1] Ann, K.Y. & Song, H.W. (2007) hloride threshold level for corrosion of steel in concrete. *Corrosion Science*, 49, 4113–4133.

[2] Arya, C., Buenfeld, N.R. & Newman, J.B. (1990) Factors influencing chloride-binding in concrete. *Cement and Concrete Research*, 20, 291–300.

[3] Diamond, S. (1986) Chloride concentrations in concrete pore solutions resulting from calcium and sodium admixtures. *Journal of Cement, Concrete & Aggregates*, 8, 97–102.

[4] Duprat, F. (2007) Reliability of RC beams under chloride-ingress. *Construction and Building Materials*, 21, 1605–1616.

[5] fib Draft Model Code (2010) fib Bulletins No. 55 and 56. International Federation for Structural Concrete, Lausanne, Switzerland.

[6] Glass, G.K. & Buenfeld, N. R. (1995) Chloride threshold levels for corrosion induced deterioration of steel in concrete. In Proc. of the *Proc. of the International Workshop Chloride penetration into concrete*, Nilsson O. and Ollivier J.P. (eds.), RILEM Publications, Vol.1, St. Rmy-les-Cheuvreuse, France, 429–439.

[7] Glass, G.K. & Buenfeld, N. R. (1997) The presentation of the chloride threshold level for corrosion of steel in concrete. *Corrosion Science*, 39(5), 1001–1013.

[8] Hunkeler, F. (2005) Corrosion in reinforced concrete structures - Chapt.: Corrosion in reinforced concrete: processes and mechanisms. H. Bohni, editor. Cambridge, UK, Woodhead Publishing Limited.

[9] ISO 13823 (2008) General Principles in the Design of Structures for Durability.

[10] Kawamura, M., Kayyali, O.A. & Haque, M.N. (1988) Effect of fly ash on pore solution composition in calcium and sodium chloride-bearing mortars. *Cement and Concrete Research*, 18, 763–773.

[11] Novák, D., Keršner, Z. & Teplý, B. (1998) Prediction of Structure Deterioration Based on the Bayesian Updating, In Proc. of the 4^{th} International symposium *Natural-Draught Cooling Towers*, Rotterdam, Balkema, 417–421.

[12] Novk, D., Voechovsk, M., Rusina, R. & Lehk, D. (2005) FReET Program Documentation – Part 2 – User Manual. Brno/Cervenka Consulting, Prague, Czech Republic.

[13] Papadakis, V.G. , Fardis, M.N. & Vayenas, C.G. (1992) Effect of composition, environmental factors and cement-lime mortar coating on concrete carbonation. *Materials and Structures*, 25, 293–304.

[14] Papadakis, V.G. Fardis, M.N. & Vayenas, C.G. (1995) Physicochemical processes and mathematical modeling of concrete chlorination. *Chem. Eng. Sci.*, 51(4), 505–513.

[15] Papadakis, V.G., Roumeliotis, A.P., Fardis, C.G. & Vagenas, C.G. (1996) Mathematical modelling of chloride effect on concrete durability and protection measures. In Proc. of *International Conference on Concrete in the Service of Mankind* (Concrete Repair, Rehabilitation and Protection edited by Dhir, R.K. & Jones M.R.), Dundee, Scotland, UK, 165–174.

[16] Pereira, C.J. & Hegedus, L.L. (1984) Diffusion and reaction of chloride ions in porous concrete. In Proc. of *8th International Symposium of Chemical Reaction Engineering*, Edinburgh, Scotland, UK.

[17] Teplý, B., Chromá, M., Rovnaník, P. and Novák, D. (2012) The role of modeling in the probabilistic durability assessment of concrete structures. In Proc. of *Life-Cycle and Sustainability of Civil Infrastructure Systems*, Strauss, Frangopol & Bergmeister (Eds). Taylor & Francis Group, London, 876–882.

[18] www.freet.cz